2016

Fabrication and Characterization of Gradient Oxide Thin Films

Gabriel Eng
Portland State University

Fabrication and Characterization of Gradient Oxide Thin Films

by

Gabriel Eng

An undergraduate honors thesis submitted in partial fulfillment of the

requirements for the degree of

Bachelor of Science

in

University Honors

and

Physics

Thesis Adviser

Dr. Zhiqiang Chen

Portland State University

2016

ACKNOLEGEMENTS

This work was supported by the Center for Electron Microscopy and Nanofabricaton (CEMN) at Portland State University, a signature facility of the Oregon Nanoscience and Microtechnologies Institute (ONAMI). I would like to thank my advisor, Dr. Zhiqiang Chen for insights into material science and training in electron microscopy. Thanks to Matthew Hughes for FIB training and Greg Baty for PVD training. I would like to thank Candice, Bill, and Miss Rebecca for all the support along the way.

ABSTRACT

Photovoltaic (PV) solar cells are a promising renewable energy source but the ratio of efficiency over cost of manufacture must be optimized in order to compete with traditional fossil fuel based energy sources. Much attention has been given to CuO-based thin film oxide cells because of low cost, however, their efficiency needs further improvement. In this thesis, we intend to fabricate a multi-band gap gradient Cu/SnO_x thin film targeting to enhance solar conversion efficiency. Hereojunctions of gradient Cu/SnO_x thin film were fabricated by physical vapor deposition (PVD) and followed by heat-treatment. The microstructures of the junctions were characterized by scanning transmission electron microscopy (STEM) with energy dispersive X-ray spectrometry (EDX). The formation of gradient films was demonstrated at a heat treatment of 300˚C for 15 minutes. Longer heat treatment time leads to form a uniform and saturated CuO-SnO_x alloyed thin film. We found saturated composition is correspondent with 10 at. % Cu. Little Sn was diffused into the Cu or CuO layer. This is caused by the high diffusion rate of Cu in SnO_x than that of Sn in the Cu/CuO layer.

Keywords: Band Gap Engineering, Solar Cell, Oxide Thin-Films

TABLE OF CONTENTS

TABLE OF FIGURES

TABLE OF TABLES

1 INTRODUCTION

1.1 Photovoltaic Solar Cell Status

Renewable energy sources such as photovoltaic (PV) solar cells promise to mitigate climate change, increase the security of the energy supply system, and provide developing countries access to affordable energy [1]. While there has been much progress towards meeting the global energy demand with an increasing percentage supplied by renewable resources, the majority of the world's energy consumption is supplied by fossil fuels. For renewable resources to make up a larger share of the global energy supply, they must be more cost effective by maximizing power output while reducing land use and cost of manufacture.

1.1.1 Power Conversion Efficiency

PV solar cells convert solar radiation into direct current electricity using semiconductors [2]. The amount of energy from sunlight reaching the Earth's surface varies with location, time of day, and weather conditions. It is useful to express it in terms of energy per unit time per unit area or power per unit area. The power output of a solar cell can be compared to the power input from the sun to provide a measure of efficiency. The efficiency η of a solar cell is given by,

$$\eta = \frac{P_{out}}{\frac{P_{in}}{A}A_c},$$

where P_{out} is the power output of the device, $\frac{P_{in}}{A}$ is the energy delivered by the light source per second per unit area, and A_c is the surface area of the cell. Maximizing

efficiency is a major focus in PV research as more efficient cells require less area per unit output power, leading to less raw material consumption and less land use. Efficiencies of various solar cells are shown in Table 1.

Table 1: Theoretical, possible and obtained conversion efficiencies of various solar cells [1].

Cells	Theoretical efficiencies (%)	Obtained laboratory efficiencies (%)
Single Crystalline Si	28.9	24.7
Polycrystalline Si	28.9	20.3
Amorphous Si	22	14.7
Amorphous/microcrystalline Si	28	15.1
CIS	28	19.5
III-V multi-junction	58	33.8
III-V concentrator multi-junction	70	40.7
Dye-sensitized	22	11
Polymer	22	5.7
Novel conversion paths	70	

To compute power, the appropriate voltage and current must be used. The maximum voltage of a solar cell is the open-circuit voltage V_{oc} and the maximum current is short circuit current I_{sc}. While open-circuit voltage and closed-circuit current are maximums, each occurs where the other is zero resulting in no power output. It is common to use a fill factor FF to describe the ratio of maximum power or *squareness* of the curve. Fill factor can be described as [3],

$$FF = \frac{V_{MP}I_{MP}}{V_{oc}I_{sc}} = \frac{P_{max}}{V_{oc}I_{sc}},$$

where V_{MP} and I_{MP} are the voltage and current that occur at P_{max} where power is at

a maximum or the derivative of power with respect to voltage is zero [3],

$$\frac{dP}{dV} = \frac{d(IV)}{dV} = 0,$$

These values can be obtained from an IV curve. The efficiency η is then determined by [3],

$$\eta = \frac{V_{oc} I_{sc} FF}{P_{in}} = \frac{P_{max}}{P_{in}}$$

1.1.2 Photon Energy

In the case of photovoltaic cells, energy is provided by incident light. The energy (E) of a photon of light is given by [4],

$$E = h\nu = h\frac{c}{\lambda},$$

where h is Planck's constant (4.14x10^{-15} eV s), ν is the frequency of the light, c is the speed of light (3.00x10^{8} m/s) and λ is the wavelength of the light. For reference, visible light has a wavelength of 380 nm to 750 nm leading to incident photon energies of 1.65 eV to 3.26 eV[4].

1.1.3 Semiconductors and Band Gap

Band theory organizes the allowed energy levels available to electrons in a substance into energy ranges or bands (Fig. 1). The space between the top of the valence band and the bottom of the conduction band is known as band gap. It is the energy required to move an electron from the valence band to the conduction band.

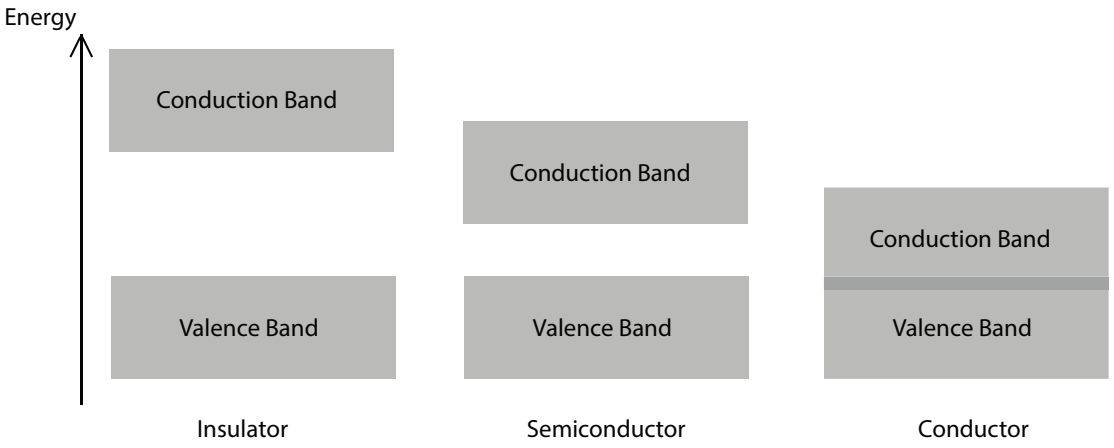

Fig. 1. Band structure of insulators, semiconductors and conductors: Insulators have a wide gap between the valence band and the conduction band while semiconductors have a smaller band gap. Conductors have overlapping valence and conduction bands.

Electrical conductors are materials whose valence band and conduction band overlap indicating electrons are free to move between the two bands. Insulators have a wide band gap between their valence and conduction bands indicating that electrons will not easily pass between the two. Semiconductors, however, only require a small amount of energy to move an electron from the valence band to the conduction band effectively turning them from insulators to conductors [4]. Solar radiation is primary in the ultraviolet to infrared and radio spectral regions with wavelengths of 0.2 to 3 μm [5] yielding energies from 0.4 to 6.2 eV. Forming materials that are sensitive to energies of specific wavelengths of light requires matching band gaps of materials to photon energies. Multi-band gap devices aim to increase responsiveness across the spectrum.

1.2 Challenges for PV Research

Challenges for PV research include the reduction of consumption of silicon and other materials in conventional crystalline silicon applications, achieving higher

efficiency models for thin-film applications, and the development of high quality transparent conductive oxides. Cost reductions will be achieved through higher efficiency, less material consumption, application of cheaper materials, innovations in manufacture, mass production and optimized system technology [1]. A primary challenge is the expense of construction of solar cells and toxic elements present in some designs [5].

The more efficient cells face the challenges of high production cost or else the use of toxic materials. The lower cost, less toxic cells face the challenge of lower efficiencies.

1.3 Common Types of Solar Cells

1.3.1 Crystalline Silicon Solar Cells

The majority of PV modules on the market are based on crystalline silicon. They fall into two main categories: single crystalline and polycrystalline. Single crystalline silicon cells have higher efficiencies but cost more to produce. Poly crystalline silicon cells are less expensive but have lower efficiencies [2][6]. Current PV module cost for single and polycrystalline silicon cells are $0.70 US/watt [7].

1.3.2 III-V Concentrator Multi-Junction Solar Cells

The highest efficiencies achieved by PV cells are achieved by III-V cells. III-V solar cells are made from compounds of elements from groups III and V of the periodic table. Most employ combinations of Gallium, Indium, and Arsenic. III-V production faces the challenge of a limited global supply of raw materials.

Concentrator III-V cells seek to overcome this challenge by focusing light on to smaller cells reducing the amount of cell area required [8]. Concentrator photovoltaic (CPV) systems use only the direct component of incoming light and require higher values of direct normal irradiation (DNI) [7]. Multi-junction cells are composed of a series of sub cells with different band gaps connected in a way resulting in higher spectral sensitivity [9]. Commercial large-scale production of CPV systems is underway [7].

1.3.3 Sensitized Solar Cells

Sensitized solar cells form a semiconductor with a photo-sensitized anode and an electrolyte [3]. Sensitized solar cells use molecular dye, inorganic sensitizers, or quantum dots. Quantum dot (QD) sensitized cells employ band gap tuning by varying particle size [10]. Sensitized cells consist of a nanoparticle oxide layer in contact with a monolayer of charge transfer dye. Photo excitation of the transfer layer promotes injects an electron into the conduction band of the oxide layer [11]. While having lower efficiencies than other technologies, they are tolerant of impurities allowing for inexpensive non-vacuum low temperature manufacturing processes such as screen printing, spraying, and pressing. Also they make use of inexpensive materials. Development of dye-sensitized solar cells faces challenges of improved efficiency and cell stability [12]. Dye-sensitized solar cells are currently limited to a research and development phase [7].

1.3.4 Thin Film Solar Cells

Thin film solar cells are formed by depositing thin layers in the micrometer range of photosensitive materials. Thin films have the advantage of low

consumption of raw materials and relative ease of manufacture [2]. Commercially produced thin film cells include amorphous silicon (a-Si), copper indium gallium di-selenide (CIS/CIGS), and Cadmium Telluride (CdTe) Cells [7].

1.4 CuO_x and SnO_x Thin Films

Metal oxide semiconductors are widely used in commercial applications such as transistors or transparent conducting electrodes. Metal oxides solar cells have received much attention due to their inexpensive materials and production methods [13]. While metal oxide semiconductors are promising and attractive for their low price of source materials and production, many designs suffer from low efficiency [14]. Hetero thin films junctions with multi band gaps have potential to improve the efficiency of solar energy absorption [15]. CuO and Cu_2O, p- type semiconductors with band gaps of ~1.5 eV and ~2.0 eV respectively, have been materials of interest due to relatively high optical absorption and low cost [15]. CuO has a monoclinic crystal structure with the following lattice parameters: a = 4.6837 Å, b = 3.4226 Å, c = 5.1288 Å, $\beta = 99.54^\circ$ [16]. Cu_2O has a cubic structure with lattice parameters a = 4.27 Å at p = 0 GPa, a = 4.18 Å at p = 10 GPa [17]. SnO_2, an n-type semiconductor with a band gap of ~3.7 eV, is of interest because of its high optical transparency and relatively low electrical resistance [18][19]. SnO_2 has a tetragonal crystal structure with lattice constants: a = 4.746 Å and c = 3.176 Å [20]. CuO_x/SnO_x junctions have received much attention as gas sensors [21] and photo detectors [22]. Transparent conducting oxides (TCO's) have received much attention for applications such as solar cells, organic light emitting diodes and flat panel displays, but in efforts to lower resistance and increase durability, metal/TCO junctions

gained increased attention [23]. Cu, CuO, and Cu_2O have long been studied for their semiconductor properties. Cu metal is highly conductive, while Cu and CuO have band gaps in the visible and near infrared regions, making them attractive for solar applications [24]. CuO_x is promising because of its non-toxic nature, abundance, and inexpensive processing [25].

Considerable efforts have been put to improve the efficiency of CuO thin films. Kidowaki fabricated ITO/CuO/C_{60} junctions with an efficiency of 1.8×10^{-6} [15]. Motoyoshi fabricated junctions of FTO/CuO/C_{60} achieving an efficiency of 2.3×10^{-4} [26]. Mittiga achieved higher efficiencies (2 %) with a heterojunction of ITO/ZnO/Cu_2O [13]. These efficiencies are still too low to be commercially competitive.

Researchers have studied methods such as nanowire growth [24], doping [27], and nano cluster growth [22].However, to our best knowledge, little work has been done to form multi-band gap single junctions of oxide thin films. To improve efficiency of CuO_x solar cell, we intend to form a multi-band gap gradient Cu/SnO_x thin film.

1.5 Research Objectives

In general, inter-diffusion as a result of heat treatment is considered an adverse effect. The question is if we could take advantage of it to fabricate the gradient alloyed thin films via control the heat treatment temperature and time, subsequently form multiband gap films (Fig. 3). As the initial step, the thesis is focused on the identification of the Cu/SnO_x gradient thin film fabrication

parameters. Scanning transmission electron microscopy with an energy dispersive x-ray spectrometer and focused ion beam microscopy are used to prove the concept.

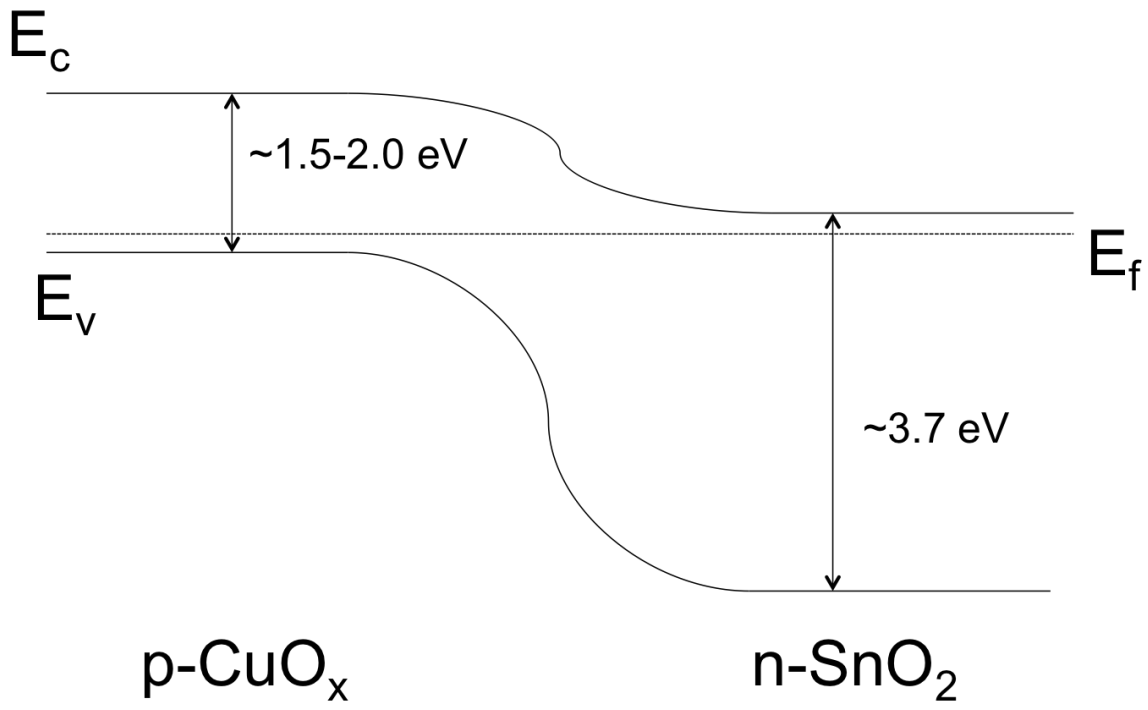

Fig. 2. Band diagram for CuO_x/SnO_2 interface. Creating a gradient diffusion layer of alloyed CuO_x/SnOx may lead to a tunable band gap material at the interface.

2 EXPERIMENT

2.1 Physical Vapor Deposition (PVD)

Physical vapor deposition (PVD) is a process of vaporizing a material and then depositing it on a substrate either through thermal evaporation or sputtering. Sputtering involves the vaporization of atoms from a surface by momentum transfer from bombarding energetic ions [28]. In this work, thin films of Cu, and SnO_x were formed on a silicon substrate by PVD in a KJ Lesker Axxis thin film deposition system. Cu was deposited at 125 W via DC sputtering and SnOx was deposited at

100 W via RF sputtering. Junctions were formed as follows. A layer (~10 nm) of SnO_x was deposited onto Si wafer to enhance Cu adhesion. Cu metal (1.1 μm) was then deposited on top of the adhesion layer. The sample was then removed from vacuum and masked with tape to leave areas of exposed Cu for electrical contact probes. The sample was then reinserted for the next layer. SnO_x (~550 nm) was deposited on the Cu over masked and unmasked regions (Fig. 3).

Fig. 3. Cu is deposited on SiO_2/Si. With some areas masked and others unmasked, SnO_x is deposited on top of the Cu layer.

2.2 Heat Treatment

Preliminary experimentation showed that Cu readily diffused into SnO_x with heat-treatment. In an effort to control this diffusion, the time in the furnace was varied. The junctions formed by PVD were heat-treated in atmosphere in a Thermo Scientific Thermolyne furnace preheated to 300˚C. The samples were inserted without ramping. They were removed from the furnace after a designated time and allowed to cool. Samples were organized into three groups: as deposited, samples heat-treated for 15 minutes at 300˚C, and samples heat treated for 60 minutes at 300˚C. Thermal oxidation of the Cu contact points was removed with a 0.5 μm

diamond paste with a subsequent ethanol rinse to reveal a Cu metal electrical contact.

2.3 Characterization via TEM with EDX

A TEM accelerates electrons through a column and focuses them into a beam that passes through a thin sample. A TEM with scanning capability (STEM) can raster-scan a beam across a sample, and correlate detector readings to locations on the sample. A high angle annular dark field detector (HAADF) functions by detecting spatial deflection of electrons transmitted through the sample as a result of interactions with the sample.

Energy dispersive x-ray spectroscopy (EDX) is a technique which measures characteristic emission x-rays to determine the elemental composition of a material. An Inner-shell electron is excited by the electron beam to a higher energy level leaving a hole in the inner shell. As a more energetic electron undergoes a reduction in energy so as to fill the hole, the difference in energy is accounted for as an emitted photon with an energy characteristic of the transition. Many well-known transitions for different atoms are produced at energy levels within the range of a TEM's electron beam. The emitted x-ray spectra can be analyzed to determine elemental composition [29].

To characterize the junctions at the interface between layers, cross-section specimens were prepared from the thin films via a dual beam, focused ion beam (FIB) microscope. Imaging and composition analysis were performed at 200 kV on an FEI TECNAI F20 (Fig. 4) transmission electron microscope using a HAADF

detector for STEM imaging with an Oxford SDD EDX detector for elemental composition analysis.

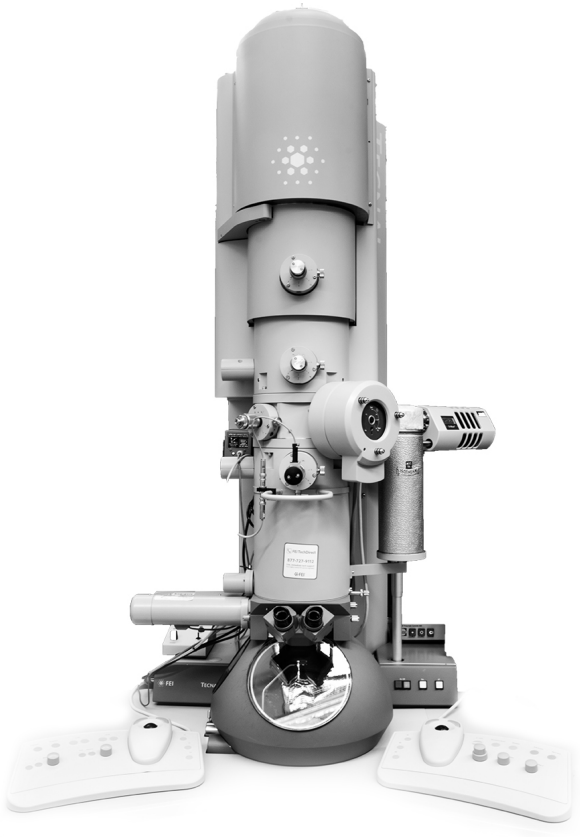

Fig. 4. An FEI Tecnai F20 TEM with an Oxford X-Max 80 mm^2 SDD EDX Detector.

Molybdenum grids (opposed to copper) and a low background double tilt holder were used to reduce background signal. EDX elemental maps and line scans corresponding to locations on the STEM images were constructed from x-ray data via Aztec software by Oxford Instruments.

Selected area electron diffraction (SAED) images were acquired via TEM in the SnO_x layer of the sample heat-treated at 300˚C for 15 minutes.

3 RESULTS

3.1 Microstructure Characteristics of the As-Deposited Cu/ SnO_x Junction

As shown in Fig 5a and b, a sharp interface can be seen between Cu and SnO_x in the STEM image with EDX maps and EDX line scan. Further composition analysis shows very little Cu signal in the SnO_x layer and very little Sn signal in the Cu layer. This low amount of Cu signal is coming from spurious x-ray on the Cu O ring. The ratio of oxygen to tin ~200 nm into the SnO_x layer is 57.7 to 38.9 (Table 2) or ~1.5 oxygen for each tin. The oxygen deficiency might be attributed to SnO_x deposition in an oxygen deficient environment under vacuum. There is no apparent inter-diffusion in the thin film layers of as-deposited samples.

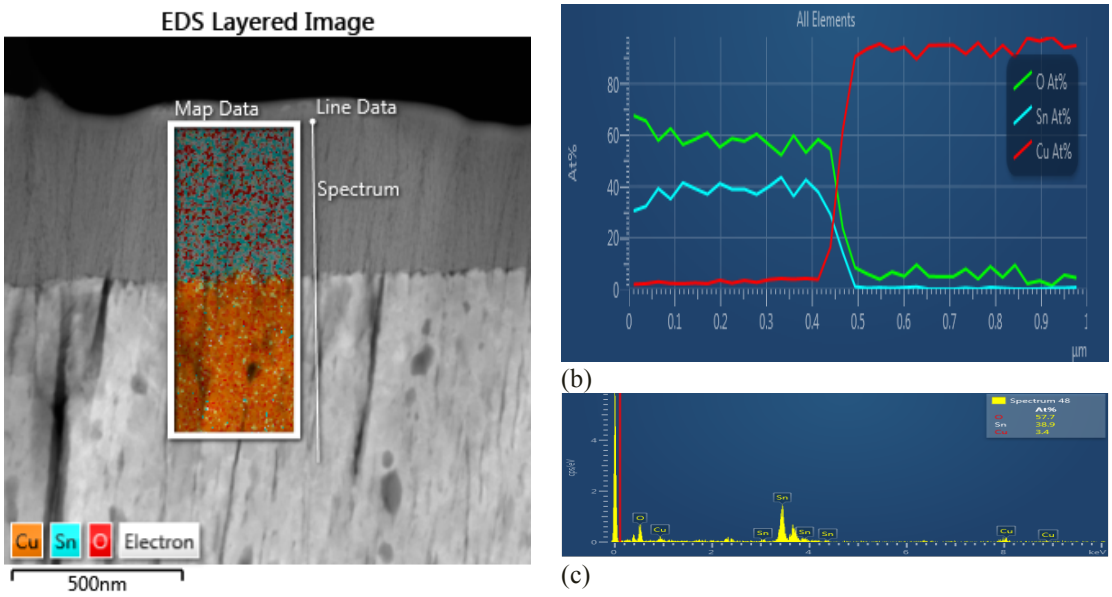

Fig. 5. Cu/SnO_x interface as deposited: HAADF STEM Image with EDX elemental map overlays (a), EDX line scan (b), and (c) EDX spectrum. The spectrum was acquired in the SnO_x layer ~200 nm from the interface. Little diffusion between the layers can be seen.

3.2 Microstructure Characteristics of the Cu/SnO_x Junction Heat-Treated at 300˚C for 15 Minutes

After heat-treated at 300˚C for 15 minutes, Cu diffused into the SnO_x layer. In comparison to the cross-section microstructure of as-deposited thin films, an apparent interfacial layer is visible between SnO_x and the Cu layer. The thickness of SnO_x layer is reduced significantly. On the interfacial layer between SnO_x and Cu, the line scanning profiles show an approximately constant concentration of Cu (10.9 at. %) for ~300 nm followed by an obvious gradient decrease to little Cu over the next ~200 nm without significant Sn composition change (Fig. 6). Above the Cu layer, Cu diffusion is visible as a light colored smooth region in the SnO_x layer. This demonstrates the formation of Cu-gradient SnO_x film on the interfacial layer.

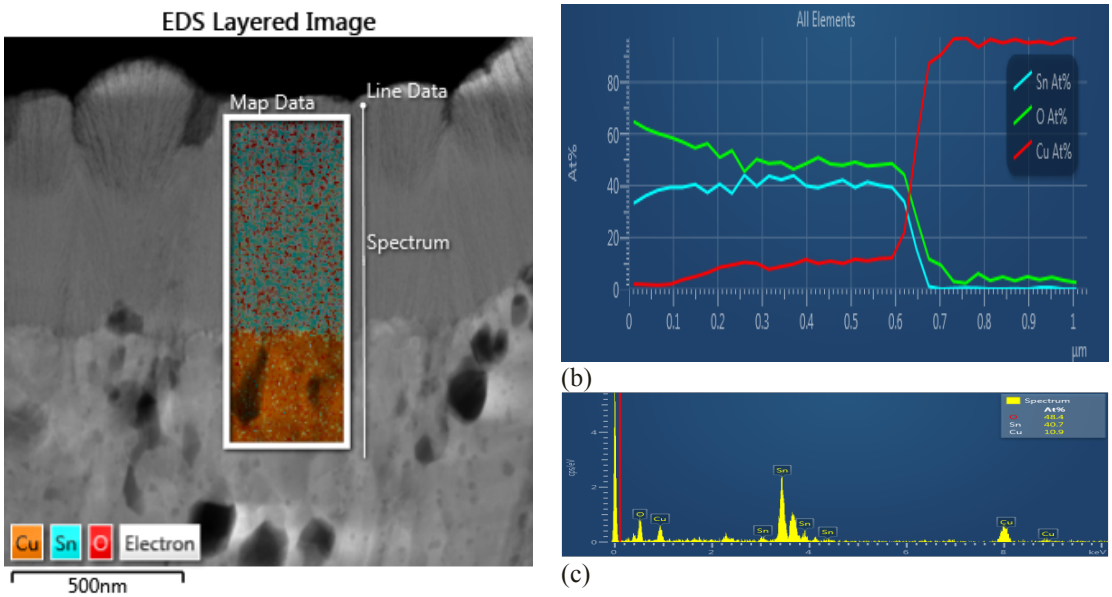

Fig. 6. STEM Image with EDX elemental map overlays (a), EDX line scan (b), and (c) EDX spectrum of Cu/SnOx interface heat treated at 300˚C for 15 minutes. Cu is diffused into the SnO_x layer with an approximately constant concentration for ~300 nm followed by a gradient decrease to pure SnO_x over ~200 nm.

An SAED pattern (Fig. 7) taken from the interfacial layer heat-treated for 15 minutes is correspondent with the SnO_x phase, which suggests that Cu diffuses into the SnO_x layer without phase transformation and leads to formation of SnO_x-Cu solid solution. It suggests that Cu can act as a dopant in SnO_x phase with proper control of heat treatment.

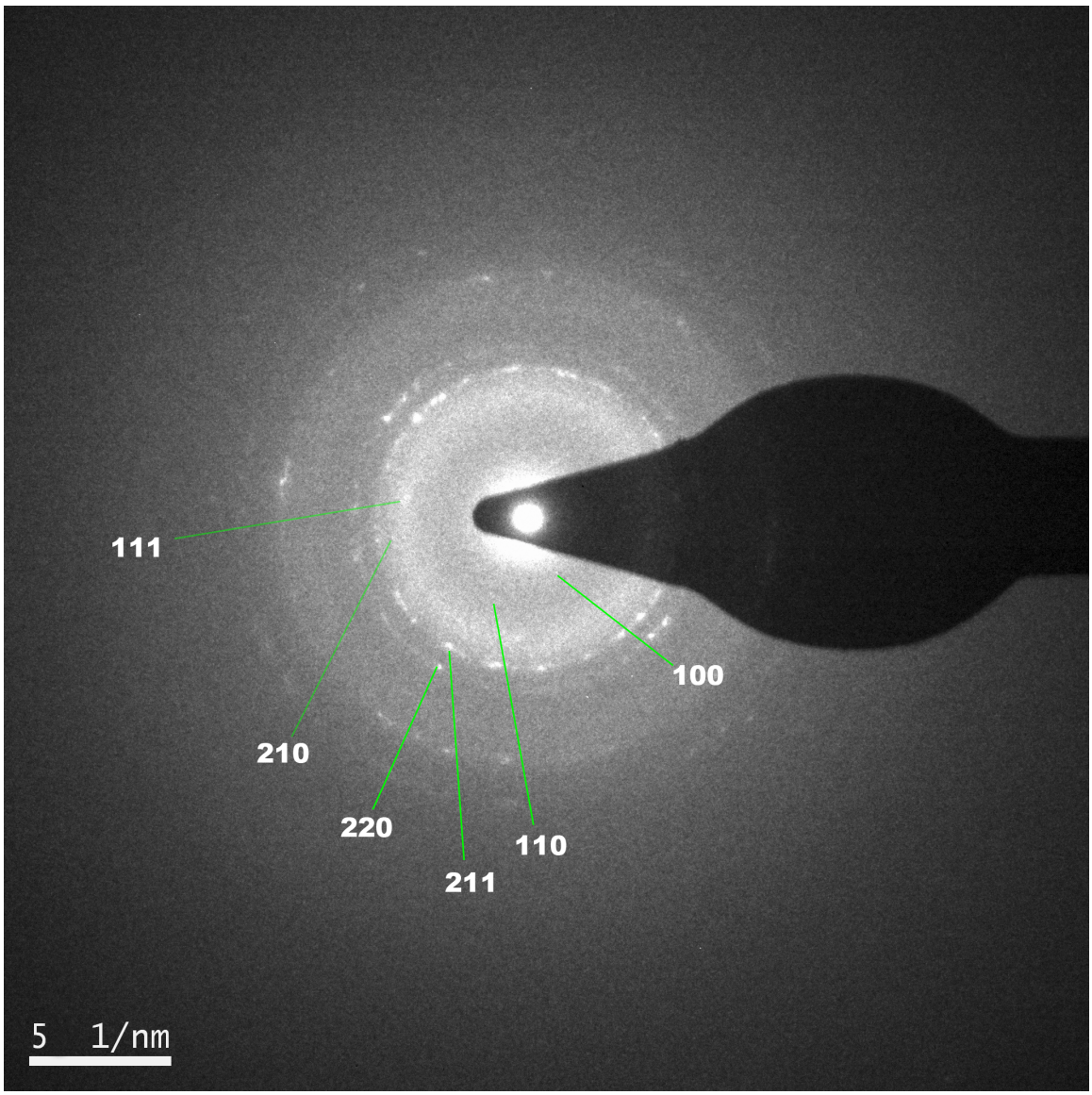

Fig. 7. Selected area electron diffraction (SAED) images acquired via TEM from the Cu-diffused SnO_x layer of a Cu/SnO_x junction heat-treated at 300˚C for 15 minutes. The d-spacings measured by SAED are consistent with those of SnO_x.

The pure SnO_x is towards the top of the layer is less smooth (Fig. 6a). The oxygen content is the highest towards the top of the SnO_x layer, which is caused by oxygen diffusion into SnO_x layer from the top surface during heat treatment. The dark contrast phase in the Cu layer is caused by the voids (dark spots in the bottom layer in Fig. 6a). Further work needs to be done to optimize the deposition of Cu.

3.3 Microstructure Characteristics of the Cu/SnO_x Junction Heat-Treated at 300˚C for 60 Minutes

The thin film heat-treated for 60 minutes shows an approximately constant concentration of Cu (10.1 to 12.5 At. %) throughout the entire SnO_x layer (Fig. 8). The Cu diffused SnO_x layer has the same smooth appearance in the STEM image as the sample heat-treated for 15 minutes, but this smooth layer continues to the top.

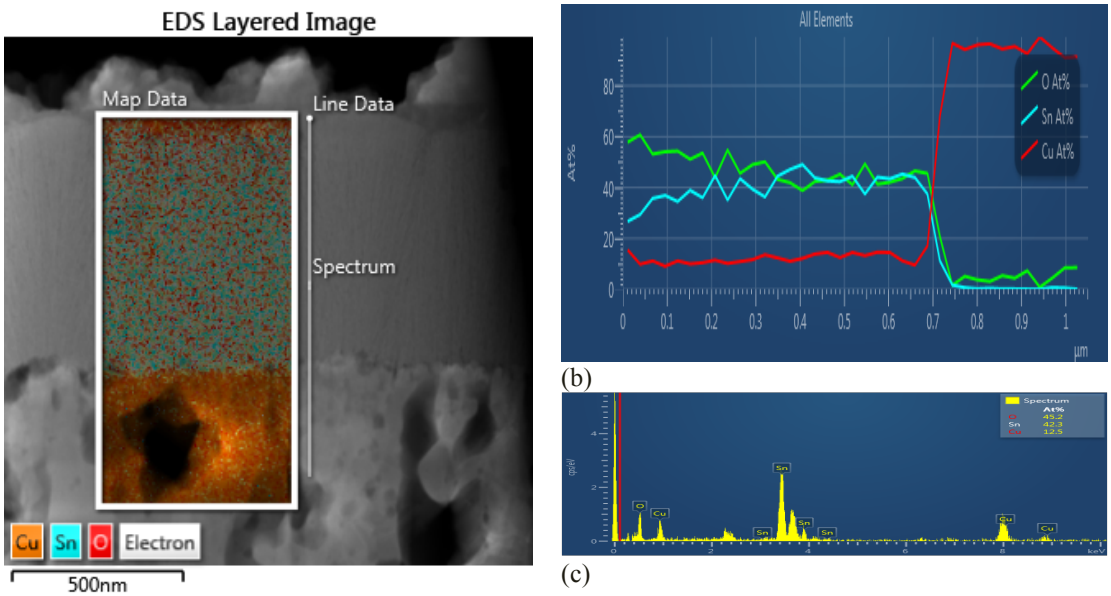

Fig. 8. HAADF STEM Image with EDX elemental map overlays (a), EDX line scan (b), and (c) EDX spectrum of Cu/SnO_x interface heat treated at 300˚C for 60 minutes. Cu is diffused into the SnO_x layer with an approximately constant concentration across the entire SnO_x layer.

It appears the Cu diffusion in SnO_x has reached a saturated concentration. Like the as-deposited sample, the oxygen content is higher towards the top of the SnO_x layer.

Table 2 shows that that the diffusion of Cu into the SnO_x layer increased with heat-treatment time and that there was no significant Sn diffusion into the Cu layer.

Table 2. Atomic concentrations of Sn, O, and Cu acquired by EDX in three locations in the Cu/SnO_x junction as-deposited, heat-treated at 300˚C for 15 minutes, and heat-treated at 300˚C for for 60 minutes.

Location	Time at 300˚C (min)	Sn (at. %)	O (at. %)	Cu (at. %)
~200 nm	0	0.0	5.0	95.0
Into Cu	15	0.1	3.4	96.6
Layer	60	0.1	4.4	95.5
~200 nm	0	38.9	57.7	3.4
Into SnO_x	15	40.7	48.4	10.9
Layer	60	42.3	45.2	12.5
~450 nm	0	32.3	65.5	2.2
Into SnO_x	15	37.3	56.3	6.4
Layer	60	35.1	54.8	10.1

As a summary, we have found that

1) With proper heat-treatment, Cu readily diffuses into SnO_x without phase transformation, but little Sn diffuse into Cu.

2) By controlling heat-treatment, SnO_x-Cu gradient can be formed.

3) Cu reaches a saturated concentration of ~10 at. % in SnO_x.

4 CONCLUSION

SnO_x-Cu gradient alloy thin film can be fabricated via a simple thermal treatment. Future work would include variation of experimental parameters to tune the diffusion process and study the effects on the band structure of the heterojunctions. The effects of porosity, and crystallization of the SnO_x layer require more examination. Photovoltaic testing is needed to study the efficiencies of cells fabricated with this method..

5 REFERENCES

[1] Andrew Blakers et al., "Research and Development on Renewable Energies - A Global Report on Photovoltaic and Wind Energy." International Science Panel on Renewable Energies, 2009.

[2] Y. Chu, "Review and comparison of different solar energy technologies," *Glob. Energy Netw. Inst. GENI San Diego CA*, 2011.

[3] R. Serway, C. Moses, and C. Moyer, *Modern physics*. Cengage Learning, 2004.

[4] S. Sagadevan, "Recent trends on nanostructures based solar energy applications: a review," *Rev Adv Mater Sci*, vol. 34, pp. 44–61, 2013.

[5] A. K. Pandey, V. V. Tyagi, J. A. Selvaraj, N. A. Rahim, and S. K. Tyagi, "Recent advances in solar photovoltaic systems for emerging trends and advanced applications," *Renew. Sustain. Energy Rev.*, vol. 53, pp. 859–884, Jan. 2016.

[6] J. Khan and M. H. Arsalan, "Solar power technologies for sustainable electricity generation – A review," *Renew. Sustain. Energy Rev.*, vol. 55, pp. 414–425, Mar. 2016.

[7] Simon P. Philipps, Adreas W. Bett, Kelsey Horowitz, and Sarah Kurts, "Current Status of Concentrator Photovoltaic (CPV) Technology." Fraunhofer Institute for Solar Energy Systems ISE Germany / National Renewable Energy Laboratory USA, 2016.

[8] Marios Theristis, Eduardo F. Fernández, Cameron Stark, and Tadhg S. O'Donovan, "A theoretical analysis of the impact of atmospheric parameters on the spectral, electrical and thermal performance of a concentrating III-V triple-junction solar cell." Energy Conversion and Management, 2015.

[9] J. Tian and G. Cao, "Semiconductor quantum dot-sensitized solar cells," *Nano Rev.*, vol. 4, no. 0, Oct. 2013.

[10] M. Grätzel, "Dye-sensitized solar cells," *J. Photochem. Photobiol. C Photochem. Rev.*, vol. 4, no. 2, pp. 145–153, Oct. 2003.

[11] Rick Matson, "National Solar Technology Roadmap: Sensitized Solar Cells." US Department of Energy, 2007.

[12] M. Pavan, S. Rühle, A. Ginsburg, D. A. Keller, H.-N. Barad, P. M. Sberna, D. Nunes, R. Martins, A. Y. Anderson, A. Zaban, and E. Fortunato, "TiO2/Cu2O all-oxide heterojunction solar cells produced by spray pyrolysis," *Sol. Energy Mater. Sol. Cells*, vol. 132, pp. 549–556, Jan. 2015.

[13] A. Mittiga, E. Salza, F. Sarto, M. Tucci, and R. Vasanthi, "Heterojunction solar cell with 2% efficiency based on a Cu[sub 2]O substrate," *Appl. Phys. Lett.*, vol. 88, no. 16, p. 163502, 2006.

[14] M. Woodhouse and B. A. Parkinson, "Combinatorial approaches for the identification and optimization of oxide semiconductors for efficient solar photoelectrolysis," *Chem. Soc. Rev.*, vol. 38, no. 1, p. 197, 2009.

[15] H. Kidowaki, T. Oku, T. Akiyama, A. Suzuki, B. Jeyadevan, and J. Cuya, "Fabrication and Characterization of CuO-based Solar Cells," *J. Mater. Sci. Res.*, vol. 1, no. 1, Dec. 2011.

[16] O. Madelung, U. Rössler, and M. Schulz, Eds., “Cupric oxide (CuO) crystal structure, lattice parameters,” in *Non-Tetrahedrally Bonded Elements and Binary Compounds I*, Berlin, Heidelberg: Springer Berlin Heidelberg, 1998, pp. 1–3.
[17] O. Madelung, U. Rössler, and M. Schulz, Eds., “Cuprous oxide (Cu2O) crystal structure, lattice parameters,” in *Non-Tetrahedrally Bonded Elements and Binary Compounds I*, Berlin, Heidelberg: Springer Berlin Heidelberg, 1998, pp. 1–3.
[18] S. Baco, A. Chik, and F. Md Yassin, “Study on optical properties of tin oxide thin film at different annealing temperature,” *J. Sci. Technol.*, vol. 4, no. 1, 2012.
[19] M. Batzill and U. Diebold, “The surface and materials science of tin oxide,” *Prog. Surf. Sci.*, vol. 79, no. 2–4, pp. 47–154, 2005.
[20] A. Ayeshamariam, C. Sanjeeviraja, and R. P. Samy, “Synthesis, structural and optical characterizations of SnO2 nanoparticles,” *J. Photonics Spintron.*, vol. 2, no. 2, p. 4, 2013.
[21] A. Chowdhuri, D. Haridas, K. Sreenivas, and V. Gupta, “Mechanism of trace level H2S gas sensing using RF sputtered SnO2 thin films with CuO catalytic overlayer,” *Int. J. Smart Sens. Intell. Syst.*, vol. 2, 2009.
[22] T. Xie, M. R. Hasan, B. Qiu, E. S. Arinze, N. V. Nguyen, A. Motayed, S. M. Thon, and R. Debnath, “High-performing visible-blind photodetectors based on SnO2/CuO nanoheterojunctions,” *Appl. Phys. Lett.*, vol. 107, no. 24, p. 241108, Dec. 2015.
[23] S. Yu, L. Li, D. Xu, H. Dong, and Y. Jin, “Characterization of SnO2/Cu/SnO2 multilayers for high performance transparent conducting electrodes,” *Thin Solid Films*, vol. 562, pp. 501–505, Jul. 2014.
[24] S. Bugarinović, M. Rajčić-Vujasinović, Z. Stević, and V. Grekulović, “Cuprous Oxide as an Active Material for Solar Cells.”
[25] C.-H. Hsu, L.-C. Chen, and Y.-F. Lin, “Preparation and Optoelectronic Characteristics of ZnO/CuO-Cu2O Complex Inverse Heterostructure with GaP Buffer for Solar Cell Applications,” *Materials*, vol. 6, no. 10, pp. 4479–4488, Oct. 2013.
[26] R. Motoyoshi, T. Oku, H. Kidowaki, A. Suzuki, K. Kikuchi, S. Kikuchi, and B. Jeyadevan, “Structure and photovoltaic activity of cupric oxide-based thin film solar cells,” *J. Ceram. Soc. Jpn.*, vol. 118, no. 1383, pp. 1021–1023, 2010.
[27] E. O. Omayio, P. M. Karimi, W. K. Njoroge, and F. K. Mugwanga, “Current-voltage characteristics of p-CuO/n-ZnO: Sn Solar cell,” *Int J Thin Film Sci Tec*, vol. 2, no. 1, pp. 25–28, 2013.
[28] Donald M. Mattox, *Handbook of Physical Vapor Deposition (PVD) Processing*, 2nd ed. Elsevier, 2010.
[29] David B. Williams and C. Barry Carter, *Transmission Electron Microscopy - A Textbook for Materials Science*. Springer, 2009.